

Countering the Over-Reliance Trap: Mitigating Object Hallucination for LVLMs via a Self-Validation Framework

Shiyu Liu^{1*}, Xinyi Wen^{2*}, Zhibin Lan², Ante Wang², Jinsong Su^{1,2†}

¹Institute of Artificial Intelligence, Xiamen University

²School of Informatics, Xiamen University

Abstract

Despite progress in Large Vision Language Models (LVLMs), object hallucination remains a critical issue in image captioning task, where models generate descriptions of non-existent objects, compromising their reliability. Previous work attributes this to LVLMs' over-reliance on language priors and attempts to mitigate it through logits calibration. However, they still lack a thorough analysis of the over-reliance. To gain a deeper understanding of over-reliance, we conduct a series of preliminary experiments, indicating that as the generation length increases, LVLMs' over-reliance on language priors leads to inflated probability of hallucinated object tokens, consequently exacerbating object hallucination. To circumvent this issue, we propose **Language-Prior-Free Verification** to enable LVLMs to faithfully verify the confidence of object existence. Based on this, we propose a novel training-free **Self-Validation Framework** to counter the over-reliance trap. It first validates objects' existence in sampled candidate captions and further mitigates object hallucination via caption selection or aggregation. Experiment results demonstrate that our framework mitigates object hallucination significantly in image captioning task (e.g., 65.6% improvement on CHAIR₁ metric with LLaVA-v1.5-7B), surpassing the previous SOTA methods. This result highlights a novel path towards mitigating hallucination by unlocking the inherent potential within LVLMs themselves.¹

1 Introduction

Recent advancements in Large Vision Language Models (LVLMs) (Yin et al. 2023a) have significantly enhanced their capacity to process and interpret visual inputs, achieving remarkable performance in tasks like image captioning and visual question answering (Liu et al. 2024b; Dai et al. 2023; Bai et al. 2025). However, these models remain prone to object hallucination, where the generated textual outputs diverge from the actual visual content, including objects not existing in image, undermining their reliability (Rohrbach et al. 2018; Li et al. 2023; Lovenia et al. 2024). Addressing object hallucination is critical for real-world applications, as even minor inaccuracies can lead to misleading or nonsensical responses.

*These authors contributed equally.

†Corresponding author.

¹Code is available at <https://github.com/Liushiyu-0709/SelfVal>

Extensive research has attributed the cause of object hallucination to LVLM's inherent **over-reliance on language priors**—where generation depends solely on previously generated textual context while ignoring the image (Niu et al. 2021; Leng et al. 2024; Zhang et al. 2024). To mitigate this issue, recent work introduces logits calibration to suppress hallucinated logits or encourage factual ones. Among the most representative methods, VCD (Leng et al. 2024) contrasts output distributions derived from original and distorted visual inputs, while DeCo (Wang et al. 2025) leverages preceding-layer to correct the final output distribution. However, our empirical analysis reveals that while these methods can mitigate the over-reliance to some extent, they fail to reverse the trend of increasingly severe over-reliance as generation length grows. Consequently, their object generation decisions still overly rely on language priors, resulting in hallucinated object description.

Can we bypass this over-reliance trap to accurately estimate the confidence of object's existence? It is intuitive that answers consisting of only a single word or phrase can inherently avoid the problem, as they lack preceding generated text to rely on besides the image itself. Building on this insight, we propose a method termed **Language-Prior-Free Verification (LPFV)**. Following initial caption generation, LPFV is employed by instructing the model: “*Describe any element of the image with only one word or phrase.*” The resulting distribution provides a confidence score for each object's existence. Further experiments confirm this score is a more reliable verifier of object existence than the original object probabilities measured in caption. Consequently, LPFV serves as a powerful verifier, offering a direct mechanism to guide the improvement of factually grounded, less hallucinatory captions.

Building on these, we propose a novel **Self-Validation Framework** for mitigating object hallucination. It leverages LPFV to measure the existence confidence of objects in multiple candidate captions, offering two alternative strategies for producing final caption. The first strategy Best-of-N Selection selects one caption with the highest average confidence. The second strategy is Filter-then-Aggregate, where low-confidence object descriptions are first filtered out before the remaining reliable descriptions are aggregated to regenerate the final caption.

Extensive experiments demonstrate that self-validation

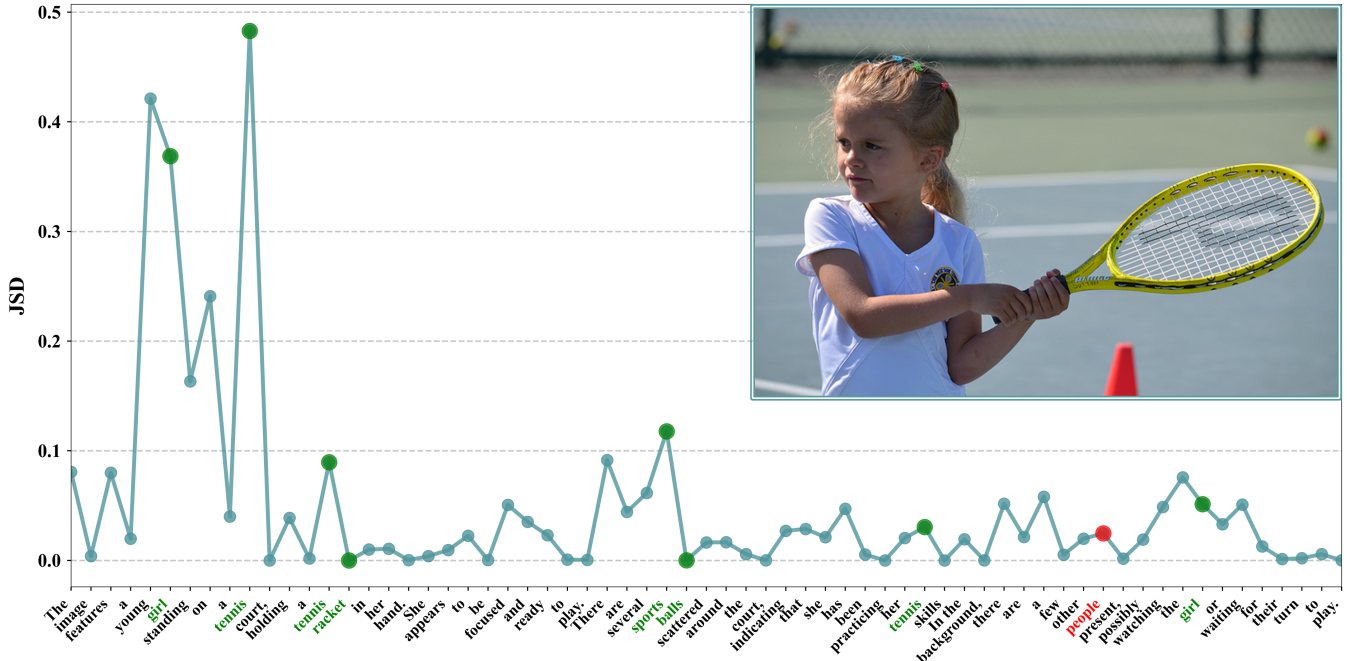


Figure 1: Illustration of JSD trend: hallucinated objects are marked in red and existent objects in green. Within the same position span, object words often exhibit higher JSD values than other words. Early-position object words yield high JSD values, whereas words in later positions consistently show low JSD values.

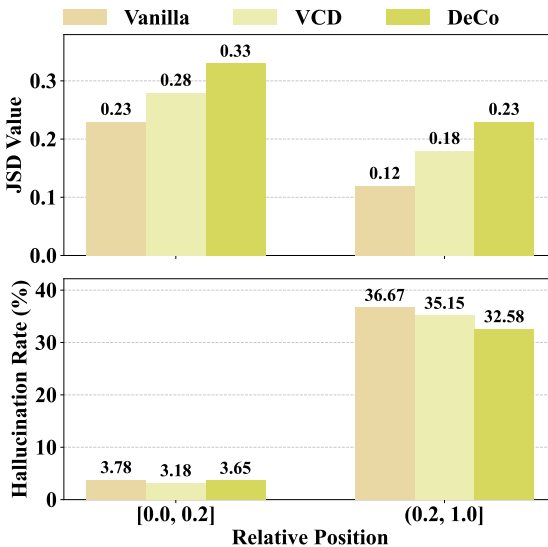


Figure 2: JSD value (top) and hallucination rate (bottom) for three methods across different relative position bins. As the generation progresses, JSD value decreases significantly, associated with a sharp increase in hallucination rate.

framework significantly reduces object hallucination in LVLMs, surpassing state-of-the-art methods by a large margin while maintaining a favorable F1 score. Its robust performance under different hyperparameter configurations and

strategy implementations validates its potential for practical applications.

2 Preliminary Study

In this section, we first conduct a series of experiments to examine LVLMs’ reliance on language priors when generating captions. Our analysis experiments are conducted in LLaVA-v1.5-7B (Liu et al. 2024b), based on samples randomly selected from the MSCOCO validation set (Lin et al. 2014).

2.1 Preliminaries for LVLM Generation

We consider an LVLM parameterized by θ . The model typically takes a textual prompt \mathbf{x} and an image \mathbf{v} as inputs, and generates a response \mathbf{y} . The response is sampled autoregressively from a probability distribution, where the generation decision at each step can be formulated as $y_t \sim p_\theta(y_t | \mathbf{v}, \mathbf{x}, y_{<t})$.

For each sampled caption \mathbf{y}_i , we can extract objects $\mathcal{O}_{\mathbf{y}_i} = \{\mathbf{o}_1, \dots, \mathbf{o}_j, \dots, \mathbf{o}_{m_i}\}$, where m_i is the total number of examined objects. Each object \mathbf{o}_j is associated with its occurrence position in the caption, denoted by $s(\mathbf{o}_j)$.

2.2 How Over-Reliance Leads to Hallucination

To quantify the impact of language priors on LVLM’s generation decision as the generation length increases, we conduct experiments to isolate the contribution of language priors to the generation decision. Specifically, for each generation step, we measure Jensen-Shannon

Divergence (**JSD**) (Lin 1991) between two distributions as $JSD(p_\theta(y_t | \mathbf{v}, \mathbf{x}, y_{<t}) \| p_\theta(y_t | \mathbf{x}, y_{<t}))$. Since taking visual input \mathbf{v} as a condition is the only difference between the two distributions, a large discrepancy indicates a high contribution of visual input \mathbf{v} , while a minor discrepancy indicates the language priors $[\mathbf{x}, y_{<t}]$ dominate the generation.

To visualize the JSD trend in generating image caption, we select a sample and plot the JSD of each word generation in Figure 1 (as a word can be decoded from multiple tokens, we assign the JSD value of its first token to the entire word). The high JSD values of object words at early positions of a sentence confirm that the LVLM focuses on image when generating these words in the initial decoding steps. However, after the first roughly 20% of decoding steps, the JSD values drop sharply. This indicates a rapid accumulation of reliance on language priors, which quickly comes to dominate the generation process.

To further investigate the relationship between JSD and hallucination rate, we divide object words into two relative-position bins: an early bin $[0, 0.2]$ and a late bin $(0.2, 1.0]$. This 0.2 threshold is chosen based on the observation that JSD typically drops sharply around this point. We randomly sample 100 instances and then calculate the average JSD and hallucination rate for each bin to analyze their correlation. In addition to the vanilla greedy decoding method, our experiments include two recently proposed representative calibration methods for mitigating reliance on language-priors: VCD (Leng et al. 2024) and DeCo (Wang et al. 2025).

As illustrated in Figure 2, the results reveal a clear inverse relationship between JSD values and hallucination rates. In the early bin $[0.0, 0.2]$, all three methods exhibit high JSD values and correspondingly low hallucination rates. However, in the late bin $(0.2, 1.0]$, the JSD values for all methods drop significantly, while hallucination rates show a tenfold increase compared to the early bin. Although the calibration methods, VCD and DeCo, successfully maintain higher JSD values than the vanilla baseline, they fail to reverse the overall downward trend. This sharp decline in JSD, coupled with the surge in hallucination, underscores a critical insight: **over-reliance on language priors exacerbates with increasing generation length, making hallucinations increasingly likely to occur toward the later position of the output.**

3 Methods

Inspired by our preceding finding, we first propose a novel verification method. Building upon this method, we then introduce a self-validation framework designed to mitigate object hallucination.

3.1 Language-Prior-Free Verification

Based on our finding that longer text generation exacerbates over-reliance on language priors, we propose **Language-Prior-Free Verification (LPFV)** to compel LVLMs to focus on the image rather than relying on previously generated text for verifying objects’ existence. As illustrated in Figure 3, we prompt the LVLMs with instruction \mathbf{x}_e :

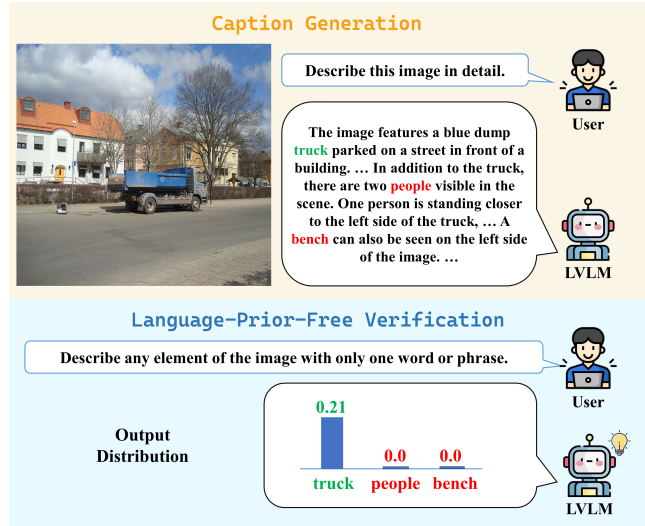


Figure 3: Hallucinated objects are highlighted in red while existent objects are in green. The LVLM provides a discriminative existence estimation of the objects when Language-Prior-Free Verification is employed, indicating that LVLMs have the ability to self-validate their generated objects.

Describe any element of the image with only one word or phrase

We expect LVLMs to output exactly one name of any existing object under the instruction \mathbf{x}_e . Compared to the **original** object probability $p_\theta(\mathbf{o} | \mathbf{v}, \mathbf{x}, \mathbf{y}_{<s(\mathbf{o})})$, **LPFV** measures object probability as $p_\theta(\mathbf{o} | \mathbf{v}, \mathbf{x}_e)$, eliminating the effect of language priors $\mathbf{y}_{<s(\mathbf{o})}$.

To compare the effectiveness of the two mentioned object probability (**original** and **LPFV**) in detecting hallucinated objects, we employ AUROC (Area Under the Receiver Operating Characteristic) for evaluation. It plots the true positive rate (TPR) against the false positive rate (FPR) at various thresholds and calculates the total area under this curve. A higher AUROC value indicates better discrimination performance, with 0.5 representing random guessing. In our experiments, the proposed LPFV method achieves an AUROC of **0.85**, whereas the original probability yields an AUROC of **0.69**.² This comparison confirms that our LPFV delivers a more reliable estimation for distinguishing between hallucinated and non-hallucinated objects, revealing LVLMs’ untapped potential when not being misled by language priors. The poor performance of the original object probability is corresponding to our finding that over-reliance on language priors leads to hallucination.

3.2 Self-Validation Framework

Based on LPFV, we introduce a self-validation framework to mitigate object hallucination in generated captions. As illustrated in Figure 4, the framework operates in two stages. In **Stage 1: Candidate Verification**, it leverages LPFV to

²We also discuss leveraging the widely used CLIPScore for verification and plot the corresponding ROC curves in Appendix.

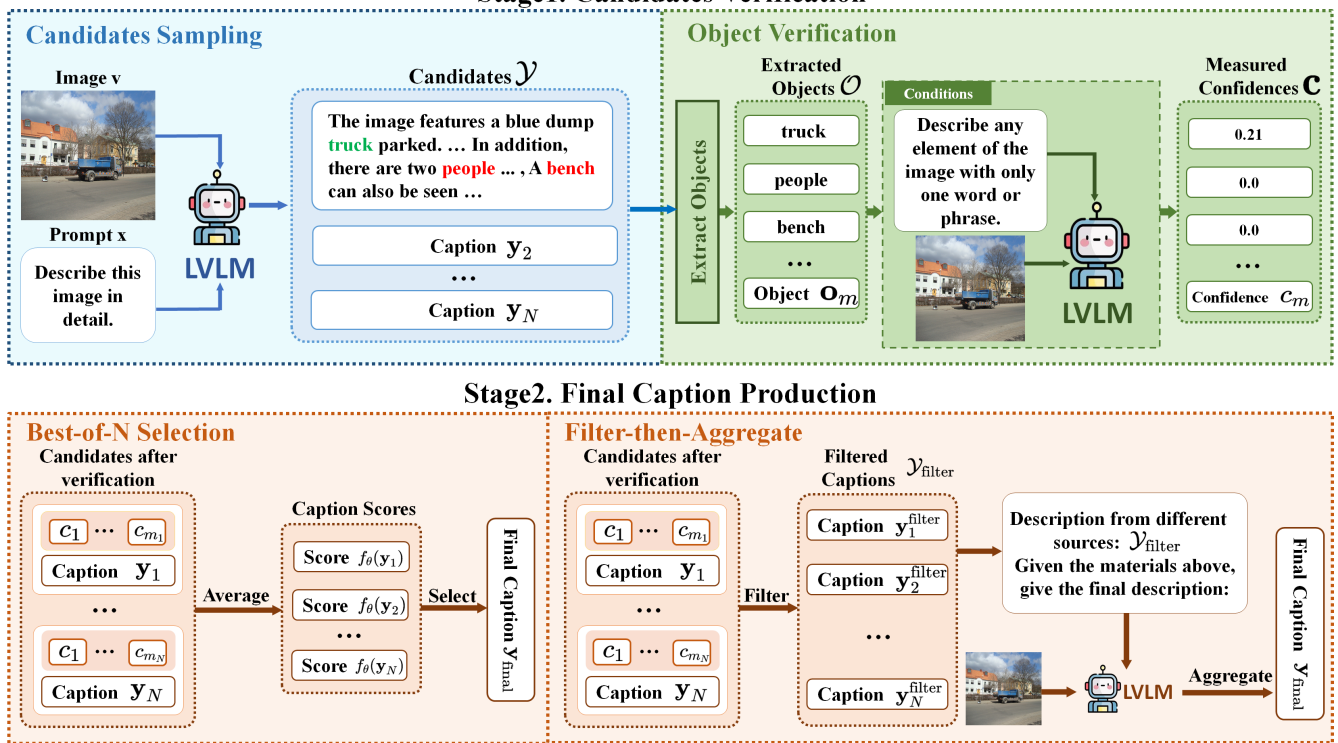


Figure 4: **Illustration of the Self-Validation Framework.** The framework operates in two stages. **Stage 1:** An LVLM first generates multiple candidate captions. For each candidate, the framework extracts objects and employs LPFV to assess their confidence scores. **Stage 2:** The final caption is produced via one of two strategies: (a) Best-of-N Selection, or (b) Filter-then-Aggregate, where sentences with low-confidence objects are discarded before aggregating the remaining content.

identify potential hallucinations among multiple candidate captions. Subsequently, in **Stage 2: Final Caption Production**, it produces more factually grounded caption using either Best-of-N Selection or Filter-then-Aggregate strategy.

3.2.1 Candidates Verification

Candidates Sampling. We follow the standard approach of sampling N captions via multinomial sampling. Each sampling process is defined as $\mathbf{y} \sim p_\theta(\mathbf{y} | \mathbf{v}, \mathbf{x})$, where \mathbf{v} is the given image and \mathbf{x} is the instruction of “*Please Describe this image in detail.*” Then, we collect N candidate captions as $\mathcal{Y} = \{\mathbf{y}_1, \dots, \mathbf{y}_i, \dots, \mathbf{y}_N\}$.

Object Verification. For each candidate caption \mathbf{y}_i , we first extract its object words $\mathcal{O}_{\mathbf{y}_i} = \{\mathbf{o}_1, \dots, \mathbf{o}_j, \dots, \mathbf{o}_{m_i}\}$. For every $\mathbf{o}_j \in \mathcal{O}_{\mathbf{y}_i}$, LPFV is employed to get corresponding confidence score $c_j = p_\theta(\mathbf{o}_j | \mathbf{v}, \mathbf{x}_e)$. The object confidences of the candidate is $\mathbf{c}_i = \{c_1, \dots, c_j, \dots, c_{m_i}\}$.

3.2.2 Final Caption Production

Best-of-N Selection. After the above steps, a direct option is to select one from the sampled candidates \mathcal{Y} as the final response $\mathbf{y}_{\text{final}}$. For each candidate \mathbf{y}_i , we average the confidence of its extracted objects as the caption-level score,

defined as:

$$f_\theta(\mathbf{y}_i) = \frac{1}{m_i} \sum_{j=1}^{m_i} c_j = \frac{1}{m_i} \sum_{j=1}^{m_i} p_\theta(\mathbf{o}_j | \mathbf{v}, \mathbf{x}_e), \quad (1)$$

where $c_j \in \mathbf{c}_i$ and $\mathbf{o}_j \in \mathcal{O}_{\mathbf{y}_i}$. Then we select the one with the highest caption-level score as the final caption.

However, we figure out that selection does not fully exploit the potential of our framework due to the following reasons: (1) The selected caption can still contain hallucinated objects. (2) The complementary factual descriptions among different candidates have not been fully utilized.

Filter-then-Aggregate. To minimize hallucinated content and fully utilize the complementary descriptions across candidates, we propose a Filter-then-Aggregate strategy for regenerating final captions.

In the filtering stage, we discard sentences containing potentially hallucinated objects (confidence score $c_j \leq \alpha$) for each candidate \mathbf{y}_i , obtaining filtered caption $\mathbf{y}_i^{\text{filter}}$. The resulting set of filtered candidates is denoted as $\mathcal{Y}_{\text{filter}}$.

Then, we prompt the LVLM to aggregate the filtered candidates to regenerate a final caption $\mathbf{y}_{\text{final}}$. The prompt for aggregation is defined as:

Row	Model	Method	Length	CHAIR _S ↓	CHAIR _I ↓	F1 ↑	Acc. ↑	Rel. ↑
1	LLaVA-v1.5-7B	-	100.6	50.0	15.4	75.1	7.50	7.89
2		VCD [CVPR24]	100.4	48.6	14.9	75.2	7.54	8.13
3		CGD [ICLR24 workshop]	89.6	37.2	11.4	78.2	7.76	8.23
4		HALC [ICML24]	72.4	32.2	10.9	69.0	6.37	6.51
5		Less [ACL24]	79.0	38.8	12.0	77.6	7.64	8.07
6		DeCo [ICLR25]	99.0	42.4	12.9	73.3	6.96	7.66
7		Nullu [CVPR25]	99.9	49.4	13.5	76.6	7.71	8.18
8		Self-Val. (w/ BoN.N=10)	98.2	28.8	7.3	76.7	7.75	8.26
9		Self-Val. (w/ FtA.N=3)	115.2	22.8	5.3	76.1	7.80	8.30
10	LLaVA-1.5-13B	-	101.0	45.8	13.0	77.0	7.65	7.29
11		Self-Val. (w/ BoN.N=10)	97.2	24.0	6.6	77.2	7.72	8.20
12		Self-Val. (w/ FtA.N=3)	121.7	21.2	5.1	76.7	7.96	8.32
13	mPLUG-Owl2-7B	-	105.8	60.8	18.9	71.6	7.28	7.66
14		Self-Val. (w/ BoN.N=10)	101.2	34.2	9.4	74.5	7.38	7.96
15		Self-Val. (w/ FtA.N=3)	98.4	13.2	4.2	70.5	7.22	7.76
16	Qwen2.5-VL-7B	-	175.3	35.6	9.9	74.4	8.52	8.70
17		Self-Val. (w/ BoN.N=10)	172.8	16.6	4.1	72.7	8.94	9.13
18		Self-Val. (w/ FtA.N=3)	156.9	8.4	3.1	70.6	8.57	8.81

Table 1: **Object hallucination performance across different methods and models on image captioning task.** Best results are in **bold**. **w/ BoN.** and **w/ FtA.** denote Best-of-N Selection and Filter-then-Aggregate. **Acc.** and **Rel.** stand for the GPT-assisted metrics Accuracy and Relevancy.

Description from different sources: $\mathcal{Y}_{\text{filter}}$
Given the materials above, give the final description:

The filtering stage enables the faithfulness of the candidate captions, and the aggregation stage can fully exploit the facts in candidates for regenerating the final caption.

4 Experiments

4.1 Setup

Models. As our self-validation framework can be seamlessly applied to any LVLMs, we choose LLaVA-v1.5 (Liu et al. 2024b), mPLUG-Owl2 (Ye et al. 2024) and Qwen2.5-VL (Bai et al. 2025) as the base models.

Baselines. To demonstrate the effectiveness of our framework, we evaluate it against SOTA decoding methods including VCD (Leng et al. 2024), CGD (Deng, Chen, and Hooi 2024), HALC (Chen et al. 2024), DeCo (Wang et al. 2025), as well as the training-based method Less (Yue, Zhang, and Jin 2024) and the editing-based method Nullu (Yang et al. 2025). All of these methods are designed for object hallucination mitigation. To ensure a fair comparison, we standardize the decoding configurations across all methods. Specifically, we set the maximum number of new tokens to 512 to guarantee complete caption generation and employ Top-k sampling with k=50 to avoid selecting low-probability tokens. The temperature is set to 0 for generation, except during the candidate sampling stage, where we apply a temperature of 0.5 to enhance diversity. We reproduce these methods to evaluate their performance; full implementation details are provided in Appendix.

Evaluation. Following previous work, we randomly sample 500 images from the MSCOCO validation set to conduct experiments (Lin et al. 2014; Yue, Zhang, and Jin 2024). Specifically, we query different LVLM models with the same prompt “*Please describe this image in detail.*”

For evaluation metric, we follow previous works (Yu et al. 2023) to use Caption Hallucination Assessment with Image Relevance (CHAIR) (Rohrbach et al. 2018). It quantifies the hallucination at both the instance level (CHAIR_I) and sentence level (CHAIR_S). These two metrics are defined as the average results of:

$$\text{CHAIR}_I = \frac{\#\text{hallucinated objects}}{\#\text{all mentioned objects}},$$

$$\text{CHAIR}_S = \frac{\#\text{captions with hallucinated objects}}{\#\text{all captions}}.$$

As the CHAIR metrics can be hacked by suppressing the richness and completeness of the captions (e.g., generating shorter or meaningless answers), we follow previous work to incorporate F1 score for evaluation (Yue, Zhang, and Jin 2024; Liu, Zheng, and Chen 2024), which is defined as:

$$\text{F1} = \frac{2 * \text{precision} * \text{recall}}{\text{precision} + \text{recall}}.$$

Since CHAIR and F1 only extract objects in captions for rule-based evaluation, we also incorporate GPT-assisted evaluation to assess overall caption quality. Specifically, we leverage GPT-4o-mini to perform a two-faceted evaluation. Each caption is scored from 1 to 10 on Accuracy (Acc.), which quantifies its factual correctness by penalizing content

inconsistent with the image, and Relevancy (Rel.), which measures the coverage of the image’s core elements and main subjects. Detailed prompt templates and scoring criteria can be found in Appendix.

4.2 Experimental Results

Experimental results in Table 1 demonstrate ours effectiveness in reducing hallucinations across LVLMs. When applied to LLaVA-v1.5-7B (Liu et al. 2024b), it achieves significant hallucination reduction (52.2%–65.6% decrease in $CHAIR_I$) across both strategies, without sacrificing the richness of the descriptions. Compared to other hallucination-mitigation methods on LLaVA-v1.5-7B, our method sets new state-of-the-art results for object hallucination. Moreover, it achieves consistent and substantial reductions in object hallucination across four LVLMs and two model sizes (7B and 13B). Regarding GPT-assisted evaluation metrics, our framework consistently outperforms the baselines.

Within our framework, Filter-then-Aggregate (FtA) always achieves a lower hallucination rate than Best-of-N (BoN) with a slight decrease in F1. This can be attributed to its mechanism of discarding descriptions of potentially hallucinated objects. However, BoN still holds an advantage on GPT-assisted evaluation in two of the four models. We hypothesize this stems from its adherence to the original distribution, thereby better preserving faithfulness. To enable a more thorough comparison between these two strategies, we provide qualitative results in Appendix.

4.3 Analysis Study

Effect of Candidates Number. Our framework involves a key parameter N , which determines the number of generated caption candidates. For the Best-of-N strategy, a larger N expands the candidate pool, increasing the likelihood of selecting captions with less hallucination. However, this may also lead to potentially overlooking captions with more rich description. For the Filter-then-Aggregate strategy, a larger candidate set provides richer descriptions for aggregation, while simultaneously introducing the risk of incorporating hallucinated content. Therefore, to thoroughly analyze the effect of N , we measure performance using both $CHAIR_I$ and recall. We evaluate both strategies with $N \in \{1, 3, 5, 10\}$ on LLaVA-v1.5-7B. For Filter-then-Aggregate, we fix the filter threshold $\alpha = 0.01$. Results are shown in Figure 5. Our key findings are as follows:

- For BoN, increasing N leads to a substantial reduction in the hallucination rate (from 50.2 to 28.8), while at the cost of a moderate decrease in recall (from 77.1 to 70.4).
- For FtA, although a larger N increases the number of description details to be aggregated (potentially raising hallucination risk), the filtering mechanism effectively prevents significant hallucination growth. Meanwhile, more candidates facilitate the aggregation of more details, thereby improving recall from 63.3 to 66.7. Notably, the performance stabilizes when $N \geq 3$.

Effect of Filter Threshold. The filter threshold α is another key hyperparameter in our framework. Specifically, we discard any sentence containing object \mathbf{o}_j , if its confidence

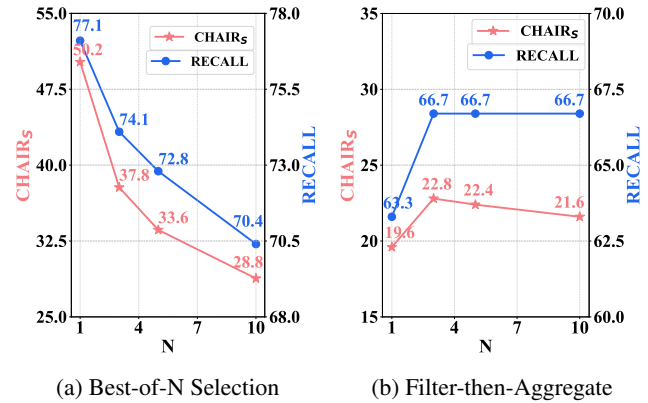


Figure 5: Impact of different candidates nums N on hallucination and recall performance.

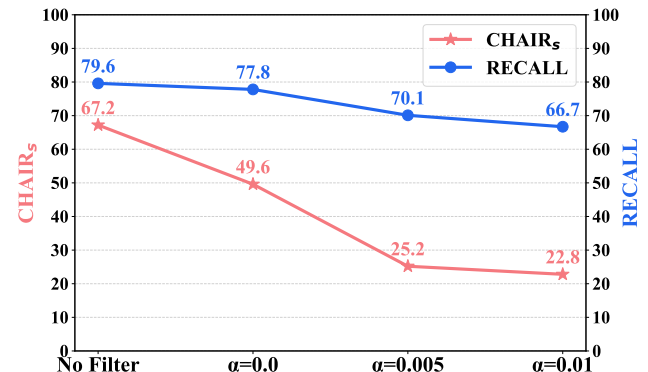


Figure 6: Impact of different filter threshold α on hallucination and recall performance.

score $c_j \leq \alpha$. We analyze the framework’s sensitivity to α across three values: $\alpha \in \{0, 0.005, 0.01\}$. Besides, we also compare these settings against a no-filter baseline that directly aggregates candidates to validate the effectiveness of our filtering mechanism. It is important to note that our Top-k ($k=50$) sampling process inherently assigns $c_j = 0$ to objects outside the top 50, meaning that $\alpha = 0$ setting already represents a basic level of filtering. All experiments are conducted with a fixed candidate number $N = 3$ (results are shown in Figure 6). Our key findings are summarized below:

- Direct aggregation without filtering exacerbates hallucination by incorporating more potentially hallucinated descriptions, highlighting the critical role of filtering.
- A higher α filters out more likely-hallucinated descriptions. This yields a substantial reduction in $CHAIR_I$ from 49.6 to 22.8, which is far more significant than the decrease in recall from 77.8 to 66.7, showing the benefit of increasing α .

Time Cost Analysis. Compared with vanilla greedy decoding, our framework incurs additional inference overhead. The extra latency stems from three sources: (1) **candidates sampling**, which is a parallelizable process; (2) **verifica-**

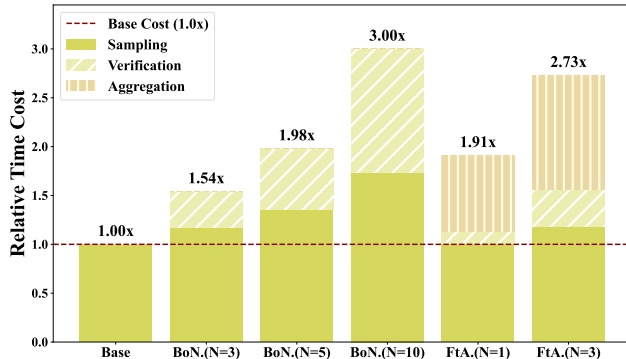


Figure 7: Time cost analysis of our framework with different values of N and strategies when applied to LLaVA-v1.5-7B.

tion, which requires a limited number of additional inference steps; and (3) **aggregation phase** unique to the FtA strategy. The time cost analysis presented in Figure 7 shows that, latency rises with the number of candidates N , and for the same N , BoN is faster than FtA.

Comparison of Object Extraction Methods. The object extraction step is crucial for our framework as it directly impacts two components: (1) candidates scoring in Best-of-N Selection and (2) sentence filtering decision in Filter-then-Aggregate. Our default implementation employs a rule-based matching approach based on a manually predefined object set derived from Rohrbach et al. (2018). This set comprises 80 common objects along with their various synonyms, yielding approximately 500 object nouns in total.

To enhance the generalization of our method for scenarios without predefined object sets, we also explore to leverage the LVLM itself for object extraction. Based on whether extraction occurs during testing, we define two modes: *offline* and *online*. For *offline* mode, we first randomly sample 2,000 captions from MSCOCO training set (Lin et al. 2014), and then prompt the LVLMs with few-shot examples to extract objects from each caption (see Appendix for prompt details). We then select the top 1,000 most common object nouns, which are used for rule-based matching during testing. For *online* mode, the LVLMs are prompted during testing to extract objects from captions.

Results of our framework under the two modes in LLaVA-v1.5-7B are presented in Table 2. The hyper-parameter setting is consistent to main experiments. Although these modes underperform the predefined object set, they remain effective at reducing hallucinations, particularly achieving comparable performance when applied to FtA. Due to the small LVLM’s limited instruction-following capability, the online extraction may lead to imprecise object extraction. This results in a less pronounced reduction in the hallucination rate compared to the offline mode. However, it gains a comparable or even better performance in GPT-assisted evaluation for its more flexible and general object extraction. Additionally, since it requires no prior in-domain data preparation, this approach offers broader applicability.

Strategy	Mode	C_S	C_I	F1	Acc.	Rel.
BoN.	<i>Online</i>	45.0	12.1	75.7	7.60	8.06
	<i>Offline</i>	41.8	10.9	75.9	7.60	8.11
FtA.	<i>Online</i>	30.4	7.6	76.5	7.45	8.02
	<i>Offline</i>	24.0	6.6	75.0	7.16	7.65

Table 2: Performance comparison of online and offline extraction modes across the two caption production strategies on LLaVA-v1.5-7B.

5 Related Work

5.1 Causes of LVLM Hallucination

Recent studies have identified multiple factors contributing to hallucination in LVLMs. A key bottleneck lies in the visual encoder’s inability to capture fine-grained details, restricting LVLMs’ capacity for accurate visual details understanding (Jiang et al. 2023; Tong et al. 2024; Wang et al. 2023). Another source of hallucination arises from the inherent bias in LVLMs. Models tend to generate high-confidence responses based on language priors or statistical bias rather than visual evidences (Zhou et al. 2023; Leng et al. 2024; Liu, Zheng, and Chen 2024). Additionally, Yue, Zhang, and Jin (2024) find that overly detailed training data hinders LVLMs’ end-of-sequence (EOS) decision ability, resulting in hallucinated descriptions.

5.2 Mitigating Hallucination for LVLMs

Recent work on mitigating hallucinations in LVLMs can be categorized into three kinds: training-phase strategies, decoding-stage strategies, and post-hoc correction. Training-phase strategies primarily focus on improving model optimization objectives or constructing more robust training datasets. Notably, Zhao et al. (2023) and Fu et al. (2025) leverage specialized DPO variants, while Yue, Zhang, and Jin (2024) propose selective EOS supervision for training. Liu et al. (2024a) construct robust visual instruction dataset for mitigating hallucination. Current decoding strategies for hallucination mitigation primarily focus on suppressing hallucinatory logits or enhancing truthful logits through calibration. As a prominent approach, contrastive decoding deliberately transforms inputs to induce hallucinations and then contrast them (Leng et al. 2024; Zhang et al. 2024; Huo et al. 2025), while Wang et al. (2025) utilize the logits from lower-layer to calibrate the final logits. Other work adapts post-hoc correction to rectify hallucinated content in model outputs. Zhou et al. (2023) utilized a trained revisor, while Yin et al. (2023b) integrates external detection models, aiming to improve the generated caption. Compared to existing work, our framework is the first to unlock LVLMs’ ability to detect and improve hallucination through overcoming the over-reliance on language priors.

6 Conclusions

In this paper, we conduct a systematic analysis of the fundamental cause of hallucinations in LVLMs—over-reliance on language priors, finding that this problem becomes more

severe as generation length increases. To counter this over-reliance trap, we propose a novel strategy to accurately estimate object confidence scores. We further integrate it into our self-validation framework to produce final captions with less hallucination. Experiments demonstrate that our framework achieves state-of-the-art performance in object hallucination mitigation.

References

Bai, S.; Chen, K.; Liu, X.; Wang, J.; Ge, W.; Song, S.; Dang, K.; Wang, P.; Wang, S.; Tang, J.; Zhong, H.; Zhu, Y.; Yang, M.; Li, Z.; Wan, J.; Wang, P.; Ding, W.; Fu, Z.; Xu, Y.; Ye, J.; Zhang, X.; Xie, T.; Cheng, Z.; Zhang, H.; Yang, Z.; Xu, H.; and Lin, J. 2025. Qwen2.5-VL Technical Report. *arXiv*.

Chen, Z.; Zhao, Z.; Luo, H.; Yao, H.; Li, B.; and Zhou, J. 2024. HALC: Object Hallucination Reduction via Adaptive Focal-Contrast Decoding. In *ICML*.

Dai, W.; Li, J.; Li, D.; Tiong, A. M. H.; Zhao, J.; Wang, W.; Li, B.; Fung, P.; and Hoi, S. C. H. 2023. InstructBLIP: Towards General-purpose Vision-Language Models with Instruction Tuning. In Oh, A.; Naumann, T.; Globerson, A.; Saenko, K.; Hardt, M.; and Levine, S., eds., *NeurIPS*.

Deng, A.; Chen, Z.; and Hooi, B. 2024. Seeing is Believing: Mitigating Hallucination in Large Vision-Language Models via CLIP-Guided Decoding. In *ICLR workshop*.

Fu, J.; Huangfu, S.; Fei, H.; Shen, X.; Hooi, B.; Qiu, X.; and Ng, S. 2025. CHiP: Cross-modal Hierarchical Direct Preference Optimization for Multimodal LLMs. In *ICLR*.

Huo, F.; Xu, W.; Zhang, Z.; Wang, H.; Chen, Z.; and Zhao, P. 2025. Self-Introspective Decoding: Alleviating Hallucinations for Large Vision-Language Models. *ICLR*.

Jiang, D.; Liu, Y.; Liu, S.; Zhang, X.; Li, J.; Xiong, H.; and Tian, Q. 2023. From clip to dino: Visual encoders shout in multi-modal large language models. *ArXiv*.

Leng, S.; Zhang, H.; Chen, G.; Li, X.; Lu, S.; Miao, C.; and Bing, L. 2024. Mitigating Object Hallucinations in Large Vision-Language Models through Visual Contrastive Decoding. In *CVPR*.

Li, Y.; Du, Y.; Zhou, K.; Wang, J.; Zhao, W. X.; and Wen, J.-R. 2023. Evaluating object hallucination in large vision-language models. In *EMNLP*.

Lin, J. 1991. Divergence measures based on the Shannon entropy. *IEEE Transactions on Information Theory*, 37(1): 145–151.

Lin, T.-Y.; Maire, M.; Belongie, S.; Hays, J.; Perona, P.; Ramanan, D.; Dollár, P.; and Zitnick, C. L. 2014. Microsoft coco: Common objects in context. In *ECCV*.

Liu, F.; Lin, K.; Li, L.; Wang, J.; Yacoob, Y.; and Wang, L. 2024a. Mitigating hallucination in large multi-modal models via robust instruction tuning. In *ICLR*.

Liu, H.; Li, C.; Li, Y.; and Lee, Y. J. 2024b. Improved baselines with visual instruction tuning. In *CVPR*.

Liu, S.; Zheng, K.; and Chen, W. 2024. Paying More Attention to Image: A Training-Free Method for Alleviating Hallucination in LVLMs. In *ECCV*.

Lovenia, H.; Dai, W.; Cahyawijaya, S.; Ji, Z.; and Fung, P. 2024. Negative Object Presence Evaluation (NOPE) to Measure Object Hallucination in Vision-Language Models. *arXiv*:2310.05338.

Niu, Y.; Tang, K.; Zhang, H.; Lu, Z.; Hua, X.; and Wen, J. 2021. Counterfactual VQA: A Cause-Effect Look at Language Bias. In *CVPR*.

Rohrbach, A.; Hendricks, L. A.; Burns, K.; Darrell, T.; and Saenko, K. 2018. Object Hallucination in Image Captioning. In *Proceedings of the 2018 Conference on Empirical Methods in Natural Language Processing*.

Tong, S.; Liu, Z.; Zhai, Y.; Ma, Y.; LeCun, Y.; and Xie, S. 2024. Eyes Wide Shut? Exploring the Visual Shortcomings of Multimodal LLMs. *ArXiv preprint*, abs/2401.06209.

Wang, C.; Chen, X.; Zhang, N.; Tian, B.; Xu, H.; Deng, S.; and Chen, H. 2025. MLLM can see? Dynamic Correction Decoding for Hallucination Mitigation. *ICLR*.

Wang, J.; Zhou, Y.; Xu, G.; Shi, P.; Zhao, C.; Xu, H.; Ye, Q.; Yan, M.; Zhang, J.; Zhu, J.; et al. 2023. Evaluation and analysis of hallucination in large vision-language models. *ArXiv preprint*, abs/2308.15126.

Yang, L.; Zheng, Z.; Chen, B.; Zhao, Z.; Lin, C.; and Shen, C. 2025. Nullu: Mitigating Object Hallucinations in Large Vision-Language Models via HalluSpace Projection. In *CVPR*.

Ye, Q.; Xu, H.; Ye, J.; Yan, M.; Hu, A.; Liu, H.; Qian, Q.; Zhang, J.; Huang, F.; and Zhou, J. 2024. mPLUG-Owl2: Revolutionizing Multi-modal Large Language Model with Modality Collaboration. In *CVPR*.

Yin, S.; Fu, C.; Zhao, S.; Li, K.; Sun, X.; Xu, T.; and Chen, E. 2023a. A Survey on Multimodal Large Language Models. *ArXiv preprint*, abs/2306.13549.

Yin, S.; Fu, C.; Zhao, S.; Xu, T.; Wang, H.; Sui, D.; Shen, Y.; Li, K.; Sun, X.; and Chen, E. 2023b. Woodpecker: Hallucination correction for multimodal large language models. *ArXiv preprint*, abs/2310.16045.

Yu, Q.; Li, J.; Wei, L.; Pang, L.; Ye, W.; Qin, B.; Tang, S.; Tian, Q.; and Zhuang, Y. 2023. HalluciDoctor: Mitigating Hallucinatory Toxicity in Visual Instruction Data. *ArXiv preprint*, abs/2311.13614.

Yue, Z.; Zhang, L.; and Jin, Q. 2024. Less is More: Mitigating Multimodal Hallucination from an EOS Decision Perspective. In *ACL*.

Zhang, Y.; Yu, W.; Wen, Q.; Wang, X.; Zhang, Z.; Wang, L.; Jin, R.; and Tan, T. 2024. Debiasing Multimodal Large Language Models. *CoRR*, abs/2403.05262.

Zhao, Z.; Wang, B.; Ouyang, L.; Dong, X.; Wang, J.; and He, C. 2023. Beyond hallucinations: Enhancing lVLMs through hallucination-aware direct preference optimization. *ArXiv preprint*, abs/2311.16839.

Zhou, Y.; Cui, C.; Yoon, J.; Zhang, L.; Deng, Z.; Finn, C.; Bansal, M.; and Yao, H. 2023. Analyzing and mitigating object hallucination in large vision-language models. *ArXiv preprint*, abs/2310.00754.

A Different Verification Methods

A.1 ROC Curves

In addition to the original object probability and LPFV, CLIPScore could also serve as an option for measuring objects’ existence confidence. It avoids over-reliance on language priors by directly computing the cosine similarity between visual and textual representations. However, as a sentence-level metric, CLIPScore represents the image in a relatively coarse way—different objects within the same sentence are forced to share the same score. The scoring of each object can be disproportionately influenced by other object descriptions in the same sentence. Therefore, we also compute object-level CLIPScore by matching object names with the image.

As illustrated in Figure 8, our proposed LPFV strategy most accurately distinguishes between hallucinated and non-hallucinated objects, revealing the untapped potential of LVLMs once freed from misleading language priors. The poor performance of using the original object probability reinforces our finding that language priors dominate generations. Furthermore, we attribute the limited effectiveness of CLIPScore to the fundamental challenge of handling multiple objects within one image.

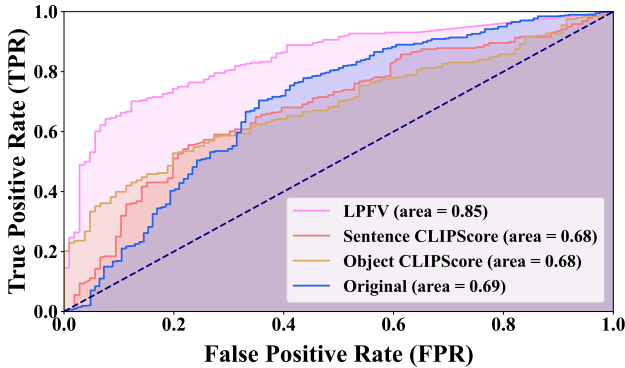


Figure 8: ROC curves of different verification methods on LLaVA-v1.5-7B. Higher AUROC indicates better performance, with 0.5 representing random guessing and 1.0 being perfect discrimination.

A.2 CLIPScore for Object Verification

To highlight the importance of the verification in our self-validation framework, we compared two methods for the object verification step: object-level CLIPScore and our LPFV. With α fixed at 0.05, we measured their respective CHAIR_I and recall scores across various N values. As shown in Figure 9, CLIPScore performs worse on both BoN and FtA, reducing hallucinations less effectively while also preserving less recall. This performance gap is explained by its weaker discrimination capability; CLIPScore achieves an AUROC of only 0.68, in contrast to 0.85 for LPFV. This result confirms that the accuracy of the verification method is critical to our framework’s overall performance.

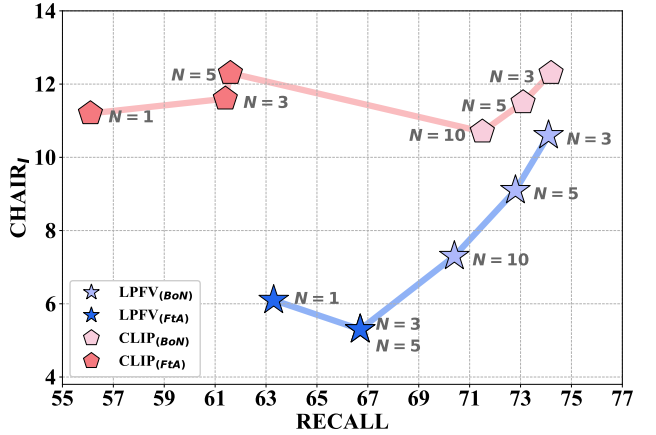


Figure 9: CHAIR_I vs. Recall performance, with CLIPScore or LPFV as object verification methods for our framework.

B Reproduction Details of Methods

B.1 Reproduction Details of Methods

We present the results of the compared methods on LLaVA-v1.5-7B in the main experiment. The hyperparameters for these methods are reported in Table 3, Table 4, Table 5, Table 6, Table 7 and Table 8, respectively. For each method, we follow the official implementation and use the configurations from their respective repositories to reproduce.

Parameters	Value
α	1
β	0.1
Noise Step	500

Table 3: VCD Hyperparameter Settings

Parameters	Value
α	0.01
β	1
Beam Size	1
Return Sequences Nums m	3
Max Candidate Nums n	3

Table 4: CGD Hyperparameter Settings

Parameters	Value
Beam Size	2
Candidate Nums k	2
Box Threshold	0.45
Expand Ratio λ	0.6

Table 5: HALC Hyperparameter Settings

Parameters	Value
Lora α	256
Lora r	128
Batch Size	64
Epoch	1
Learning Rate	$2e^{-4}$
Scheduler	cosine

Table 6: Less Hyperparameter Settings

Parameters	Value
α	0.6
Beam Size	1
Start Layer	20
End Layer	28

Table 7: DeCo Hyperparameter Settings

Parameters	Value
α	1
Top Ranks k	4
Lowest Layer	16
Highest Layer	32

Table 8: HALC Hyperparameter Settings

B.2 Object Extraction

The template for object extraction by LVLM itself is illustrated in Figure 10.

B.3 GPT-Assisted Evaluation Template

The template for the GPT-assisted evaluation is illustrated in Figure 11. To mitigate position bias (e.g., GPT favoring answer1), we alternate the order so the base caption and each method’s caption swap places as answer1 and answer2. The base model’s final score is the average of its ratings across all pairings.

C Qualitative Results

We provide qualitative demonstrations of our framework’s two strategies applied to LLaVA-v1.5-7B. Figure 12 compares the Best-of-N Selection strategy against the baseline, while Figure 13 presents the same comparison for the Filter-then-Aggregate strategy. In both comparisons, our framework clearly suppresses the object hallucinations, highlighting the effectiveness of both strategies.



Prompt

You are given a sentence, extract the objects within the sentence for me.



[Task]

1. Extract concrete physical objects from the text.
2. Exclude abstract concepts.
3. Return a JSON list with key "objects".

Here are some examples:

1. Input: He bought a bicycle and sunglasses.
Output: { "objects": ["bicycle", "sunglasses"] }
2. Input: "The idea of freedom filled the room."
Output: { "objects": [] }
3. Input: The scene also includes a dirt road and a metal gate.
Output: { "objects": ["road", "gate"] }

Now process this new input:

Input: "{caption}"

Output:

Figure 10: Prompt template for object extraction.



System Prompt

You are required to evaluate two AI assistants' image descriptions based on the actual image content.



Prompt

[Evaluation Criteria]

1. Accuracy: Check for hallucinated content inconsistent with the actual image (score 1-10)
2. Relevancy: Coverage of the image's core elements (score 1-10)

[Assistant1 Description]

{answer1}

[Assistant2 Description]

{answer2}

[Required output format]

Accuracy: <assistant1_score> <assistant2_score>

Reason: Accuracy evaluation rationale...

Relevancy: <assistant1_score> <assistant2_score>

Reason: Relevancy evaluation rationale...

Figure 11: Prompt Template for GPT-Assisted Evaluation.

**Baseline:**

The image features a dining table with a variety of donuts and pastries displayed on it. There are several donuts of different shapes and sizes, with some placed closer to the edge of the table and others in the middle. A box of donuts is also present, adding to the assortment.

In addition to the donuts, there are two cups on the table, one near the left side and the other near the right side. A person can be seen in the background, possibly enjoying the delicious treats or preparing to eat them. A chair is also visible in the scene, positioned near the left side of the table.

Ours:

The image features a table with a variety of donuts and pastries placed on top of it. There are several donuts in different flavors and styles, spread out across the table. Some of the donuts are placed closer to the edge of the table, while others are positioned near the center. A box of pastries can also be seen on the table, adding to the assortment of sweet treats.

In the background, a person is sitting in a chair, likely enjoying the delicious spread of food in front of them. The combination of donuts and pastries creates a tempting display for the person to indulge in.

**Baseline:**

The image depicts a man and a woman standing in a room filled with various suitcases and bags. The man is wearing a red jacket, while the woman is standing next to him. They appear to be looking at the luggage, possibly deciding which bags to take with them. There are numerous suitcases and bags scattered throughout the room, with some placed on the floor and others on shelves. The suitcases come in different sizes and colors, creating a diverse and visually interesting scene. The room seems to be a storage area or a place where people can choose their luggage for travel.

Ours:

The image features a room filled with numerous suitcases and bags, possibly a storage area or a room for luggage. Two men are standing among the bags, likely discussing or sorting through them. One man is standing closer to the left side of the room, while the other is positioned more toward the right side.

The room is filled with various suitcases of different sizes and shapes, some of which are placed on the floor and others on the shelves. The men are surrounded by these suitcases, making the room appear quite full.

**Baseline:**

The image features a baseball field with a man standing on the pitcher's mound, wearing a red jacket and a baseball glove. He is in the process of throwing a baseball, possibly during a game. The man appears to be the pitcher, and he is focused on his pitch.

In the background, there are two other people visible, one on the left side and another on the right side of the field. The scene captures the essence of a baseball game, with the pitcher in action and the other players ready to react to the pitch.

Ours:

The image captures a baseball pitcher in a red jacket and a blue hat, standing on a baseball field and preparing to throw a pitch. He is wearing a baseball glove, ready for the game. The pitcher is in the process of winding up for the throw, with one foot raised off the ground.

The scene takes place on a lush green field, which forms a beautiful backdrop for the baseball game. The pitcher's stance and focused expression convey the intensity and skill required for this sport.

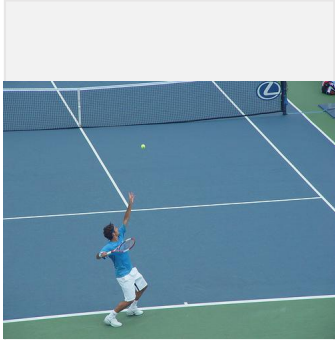
**Baseline:**

The image features a person wearing pink tights and blue shoes, standing on a carpeted floor. The person is positioned near a cat, which is sitting on the floor, possibly on a rug. The cat appears to be looking at the person's shoes, creating a sense of interaction between the person and the cat. The scene is set in a room with a chair visible in the background.

Ours:

The image features a large gray and white cat sitting on a rug, which is likely a Persian rug. The cat appears to be relaxed and content as it lays on the floor. Next to the cat, there are two blue and white shoes, possibly belonging to a person who is not visible in the image. The shoes seem to be placed at a comfortable distance from the cat, allowing for some space between them.

Figure 12: Qualitative results of the LLaVA-1.5-7B model (**Baseline**) and ours with Best-of-N Selection (**Ours**).

**Baseline:**

The image features a tennis player on a tennis court, holding a tennis racket and preparing to hit a tennis ball. The player is in the middle of a swing, with the ball positioned above his racket. The tennis ball is in the air, and the player is focused on making a successful shot.

The tennis court is surrounded by a blue net, and there is a **chair located near the edge of the court**. The scene captures the intensity and skill of the tennis player as he engages in the game.

Ours:

The image depicts a man in a blue shirt and white shorts playing tennis on a blue court. He is holding a tennis racket in his right hand and is in the process of hitting the tennis ball with a backhand swing. The tennis ball is located in the middle of the court, close to the player. The scene captures the essence of a tennis match, with the player fully engaged in the game and focused on making a successful shot. The tennis player is positioned in the center of the court, and the tennis racket is held up in a ready stance, ready to make contact with the ball.

**Baseline:**

The image features a cat sitting on a table in front of a television, watching a bird on the screen. The cat appears to be intrigued by the bird's movements, as it is focused on the television.

The television is placed on the left side of the table, and the cat is positioned on the right side. **There are several books scattered around the table, with some placed near the cat and others further away.** Additionally, there is a remote control on the table, likely used to operate the television.

Ours:

The image features a cat sitting on top of a TV stand, intently watching a bird flying on the television screen. The cat appears to be enjoying the bird's movements and is positioned on the left side of the TV. The television is placed in the center of the scene, and the cat seems to be captivated by the bird's actions. The room has a cozy atmosphere, with the TV serving as a source of companionship and entertainment for the cat.

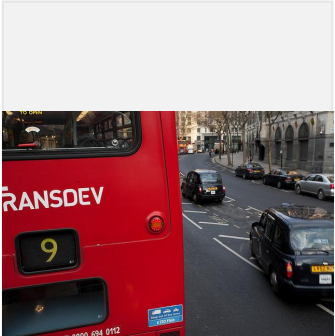
**Baseline:**

The image features a black motorcycle parked on the side of a street. The motorcycle is positioned in the middle of the scene, with its front wheel facing the viewer. The motorcycle is parked next to a car, which is visible in the background on the right side of the image.

There are two people in the scene, one standing closer to the left side of the motorcycle and the other person standing further back on the right side. The presence of these individuals suggests that they might be the owners of the motorcycle or passersby admiring the parked vehicle.

Ours:

The image showcases a black motorcycle parked on a street, with a black leather seat that adds to its sleek and stylish appearance. The motorcycle is prominently positioned in the center of the scene, occupying a significant portion of the frame. There is also a car parked towards the right side of the image, partially visible.

**Baseline:**

The image depicts a busy city street with a red double-decker bus driving down the road. The bus is surrounded by various cars, including a black car in front of it and several other cars on the street. There are also a few people walking along the sidewalk, **some of them carrying handbags.**

In addition to the vehicles, **there are two bicycles visible in the scene, one near the left side of the image and another further down the street.** The street is bustling with activity, showcasing the typical hustle and bustle of a city environment.

Ours:

The image captures a bustling city street filled with traffic, featuring a red double-decker bus driving down the road, surrounded by several cars. In front of the bus, there are multiple cars, including a black car parked on the side of the street and a few others scattered along the road. The scene is typical of a congested urban environment, with at least eleven cars visible in the image, some of which are in front of the bus and others behind it. The cars vary in size and position on the street, indicating the busy nature of the city. Additionally, **there may be pedestrians waiting to cross the street** or walking along the sidewalk, adding to the lively atmosphere of the city street.

Figure 13: Qualitative results of the LLaVA-1.5-7B model (**Baseline**) and ours with Filter-then-Aggregate (**Ours**).